

Thermoelectric Generator Based on CuSO_4 and Na_2SiO_3 †

Mihail Chira ^{1,*}, Andreea Hegyi ¹, Henriette Szilagyi ¹  and Horațiu Vermeșan ² 

¹ NIRD URBAN-INCERC Cluj-Napoca Branch, 117 Calea Florești, 400524 Cluj-Napoca, Romania; andreea.hegyi@incerc-cluj.ro (A.H.); henriette.szilagyi@incerc-cluj.ro (H.S.)

² Faculty of Material Science and Environment, Technical University of Cluj-Napoca, 103-105 Muncii Bld., 400641 Cluj-Napoca, Romania; horatiu.vermesan@imadd.utcluj.ro

* Correspondence: mihail.chira@incerc-cluj.ro

† Presented at the 14th International Conference INTER-ENG 2020 Interdisciplinarity in Engineering, Mureș, Romania, 8–9 October 2020.

Published: 18 December 2020



Abstract: Thermoelectric generators can operate at small temperature differences providing enough electricity for low-power electronics, sensors in distribution networks, and biomedical devices. The article presents the obtaining of a thermoelectric generator and its electrical characteristics using usual substances. Experimental research was carried out using a mixture consisting of several substances (copper sulfate, calcium hydroxide, silicon dioxide, and sodium silicate) in different proportions. The mixture was inserted between two plates, one graphite (hot plate) and the other aluminum (cold plate), thus obtaining a thermoelectric generator. Electrical voltage, output current, and electrical power were measured at different temperatures.

Keywords: thermoelectric generators; output current; electrical power; copper sulfate; sodium silicate

1. Introduction

The technology-based age we are in today has brought great advantages for a more comfortable and intelligent life and leads the way for even faster development in all areas of science and engineering, but at the same time brings a very high demand for energy. Current and future energy consumption requires alternative energy sources with low environmental impact. Easily available solar and wind energy have led to the use of fossil fuels as alternative energy sources [1]. Moreover, due to more recent developments in thermoelectric materials and devices (TE), the possibility of efficient use of heat energy, usually wasted, has become a feasible alternative [2]. More importantly, thermal waste has become a very important and environmentally friendly source of wasted energy [3,4]. There are already many studies explaining the mechanism of conversion of heat into electricity [5–8]. Such studies were the starting point for the development and optimization of new materials using the resources of rising nanotechnologies [9,10].

Thermoelectric devices are an attractive solution, due to their passive operation and simplicity and lack of moving parts. A thermoelectric generator is based on the Seebeck effect that generates tension in materials in the presence of a temperature gradient. Although many materials exhibit the Seebeck effect, the energy generation efficiency is based on a complex interaction between temperature, temperature gradient, Seebeck coefficient, and electrical and thermal conductivity [9]. Often, these properties do not extend in the same direction, which leads to challenges in the efficient generation of thermoelectric energy.

Altenkirch derived the thermoelectric efficiency, ZT , better known as the thermoelectric figure of merit [11], to describe the thermoelectric energy conversion capacity of a material. This value is given as

$$ZT = \frac{\alpha^2 \sigma T}{\lambda} \quad (1)$$

where α is the Seebeck coefficient, σ is the electrical conductivity, T is the absolute temperature, and λ is the thermal conductivity.

The maximum conversion efficiency of thermoelectric energy is given by the relationship:

$$\eta_{max} = \frac{T_h - T_c}{T_h} \left[\frac{\sqrt{1 + ZT_{avg}} - 1}{\sqrt{1 + ZT_{avg}} + \frac{T_c}{T_h}} \right] \quad (2)$$

Materials that offer an intrinsically high ZT value are rare and are generally composed of rare earth-based substances, in particular selenes and telluride-based alloys. SiGe alloys [4], skutterudites [12], clathrates [13], and semi-heusler alloys [14] are other promising systems, among them skutterudite, for example. p-Zn₄Sb₃, P-CeFe₃Co_{0.5}Sb₁₂, and N-CoSb₃ are actively studied by numerous research groups, providing a high value of merit in the intermediate temperature range from 500 to 973 K with conversion efficiency of 9.5% [9,15]. One approach to improving the ZT is by nano-structuring, by introducing superlattices [16] or nanostructures [17,18], since it has been recognized that it has a reduction in phononic thermal conductivity. Venkatasubramanian et al. [16] reported that the P-type Bi₂Te₃/Sb₂Te₃ superstructures exhibit an exceptionally high ZT of 2.4 at room temperature with a remarkably low thermal conductivity of 0.22 Wm⁻¹K⁻¹. There are other references to Si/Ge [19], GaAs/AlAs [20], and PbTe/PbSe [21] superstructures that have lower thermal conductivity than their alloy counterparts. However, many of these materials have low thermal and chemical stability, difficult to produce in useful forms, and are expensive, with low availability and in some cases high toxicity. There are many studies around the world to find thermoelectric potential alloys and oxides and to create multifunctional properties through microstructural engineering. The expansion of thermoelectric applicability will require the development of low-cost, abundant materials as well as the viability or applicability of scalable manufacturing technologies. A potential source of scalable thermoelectric materials is those based on transition metal oxides, which provide reasonable electrical conductivity and a Seebeck coefficient, while being cost-effective and environmentally friendly. Oxides based on Ti, Mg, W, Zn, Cu, V, Co, Rh, and Mo represent a wide range of materials, less investigated than TE materials [22]. Metal oxides can provide a wide range of electronic properties, from insulators to semiconductors.

TEG are divided into two types, large (or bulk) and micro-TEG. The first category has a millimeter size and provides the output power from several to hundreds of watts in a high heat range. This category is usually used for industrial purposes. The second category operates with low dissipated heat and generates electricity in the range of μ W up to a few mW [23].

Waste heat temperature, arrangement of TE modules, enhancing heat transfer co-efficient and parasitic loss plays an important role to maximize the net electric power [24].

In many articles, the thermoelectric material properties are assumed to be constant for easy calculation, but in fact the three properties of thermoelectricity, electrical resistivity, thermal conductivity, and Seebeck coefficient, are temperature dependent. The thermal resistance model, whose properties are assumed to be constant, overestimates the output power and efficiency of the TEG. It can be attributed to the underestimation of electrical resistance and does not solve the temperature distributions within the TEG. Assuming the properties of thermoelectric materials as a constant can induce a numerical deviation at high temperatures [25].

Waste heat recovery is very important in terms of reducing energy costs and environmental impacts. The method used for waste heat recovery must be feasible [26].

2. Materials and Methods

For the realization of the thermoelectric generator, the following materials and substances were used: graphite plate, aluminum strip, copper sulfate, sodium silicate solution of 30% concentration, calcium hydroxide, and silicon dioxide.

1.2 g CuSO_4 with 0.18 g CaOH and 0.08 g SiO_2 were mixed until homogenized, after which 2 mL of 30% Na_2SiO_3 solution was added. A homogeneous paste was obtained, which was applied to a graphite plate of 5 mm thickness, and over it was placed an aluminum strip of thickness 0.5 mm and width 30 mm. The graphite/mixture/aluminum overlap area is $50 \times 30 \text{ mm}^2$.

The obtained thermoelectric generator and the schematic representation of the layers that make up it are shown in Figure 1.

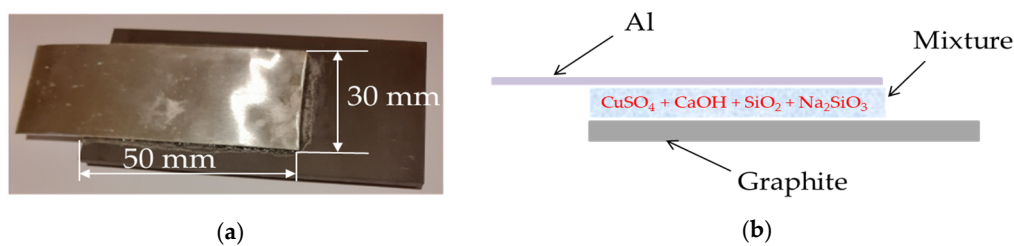


Figure 1. Thermoelectric generator made: (a) photo; (b) schematic representation.

Temperature (T_c and T_h) and electrical measurements (voltage, current, and resistivity) were performed using the digital multimeter (Peaktech P4090) from room temperature to 393 K to calculate the Seebeck coefficient, electrical conductivity, and electrical power. The Seebeck coefficient was calculated using the measured voltage generated from the temperature gradient. The temperature difference between the hot and cold part of the sample was generated by heating the graphite plate and cooling the aluminum strip, using an 800 W thermostat hob as a heater and cold air gun as a cooler.

Electrical resistivity was measured by the four-point probe technique, from room temperature to 393 K. The Open circuit was made to measure voltage and current as a temperature function to calculate power.

The thermal conductivity of the TE material was measured using a flash laser analyzer from room temperature up to 393 K.

3. Results and Discussion

The dimensions characterizing the thermoelectric generator are presented in Table 1 and Figure 2.

Table 1. Parameters of the thermoelectric generator at 393 K.

Properties at 393 K	α (mV/K)	σ (S/m)	λ (W/mK)	ZT	η (%)
Graphite/mixture/aluminum	4.3	3.3	0.875	0.027	0.129

Analyzing the data in the table, a high Seebeck coefficient is observed due to the possible p–n junctions formed between the elements of the mixture and a reasonable thermoelectric performance. Further experimental research will make it possible to improve TEG parameters by changing the percentages of substances that make up the mixture.

The Seebeck coefficient allows us to calculate the merit factor ZT and determine the efficiency of the thermoelectric generator η .

The heat source touches the graphite plate, which becomes the positive electrode, and the aluminum plate becomes the negative electrode (Figure 3).

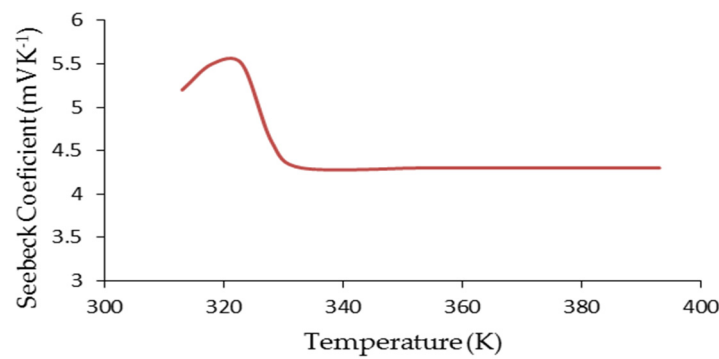


Figure 2. Seebeck coefficient of graphite/mixture/aluminum system as a function of temperature.

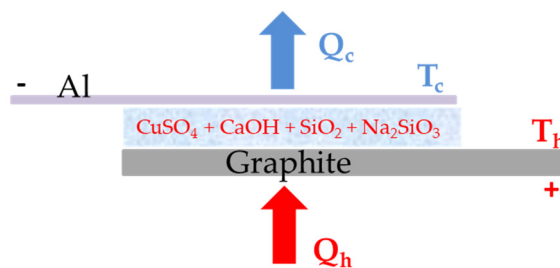


Figure 3. Schematic representation of the mode of operation of the thermoelectric generator.

The temperature of the graphite plate was increased from 297 to 393 K, and at the same time, the voltage and the output current were measured. The graphic representation of the voltage and current variation as a function of temperature can be seen in Figure 4.

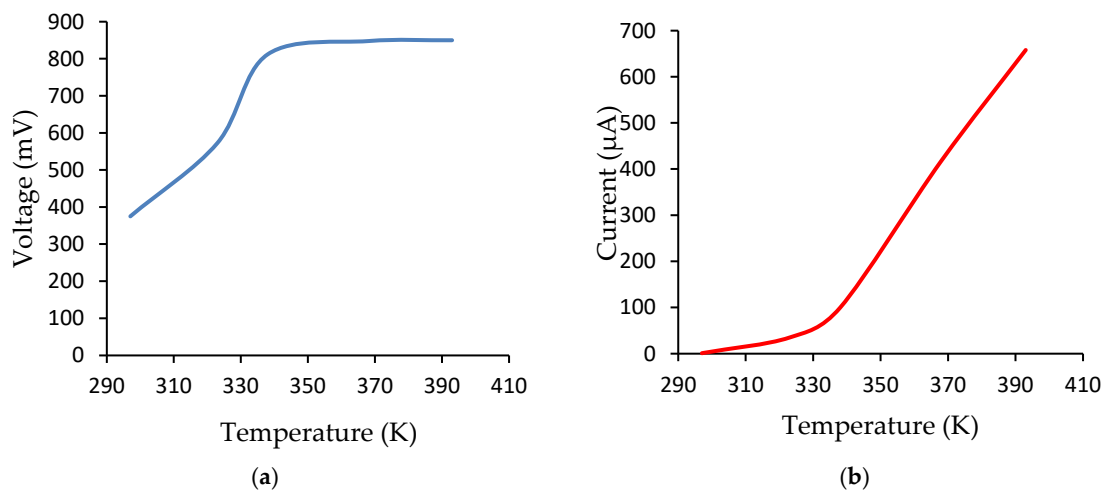


Figure 4. Thermoelectric generator: (a) the voltage; (b) the output current.

The output voltage ranges from 375 to 850 mV in the range 297–393 K, and the output current ranges from 1 to 658 μA in the same temperature range.

Analyzing Figure 4, it is found that from 330 K, the system is activated so that the output voltage reaches a maximum value around 850 mV and remains constant, and the output current has a linear increase, the slope of the line being high.

A doubling of the amount of calcium hydroxide in the mixture between the graphite and aluminum plates causes a decrease in the current three times, and a doubling of the amount of silicon dioxide causes a decrease in the current two times.

It was found that the lack of calcium hydroxide in the mixture causes a fluctuation of the generated electric current and voltage.

Serial connection of thermoelectric generators causes the Seebeck voltage to increase, while parallel connections allow the output current to increase. The combination of Serial and parallel connections should lead to an increase in both voltage and electric current.

The output voltage and current were represented according to the number of modules connected in series, respectively, in parallel to a temperature gradient of 96 K in Figure 5.

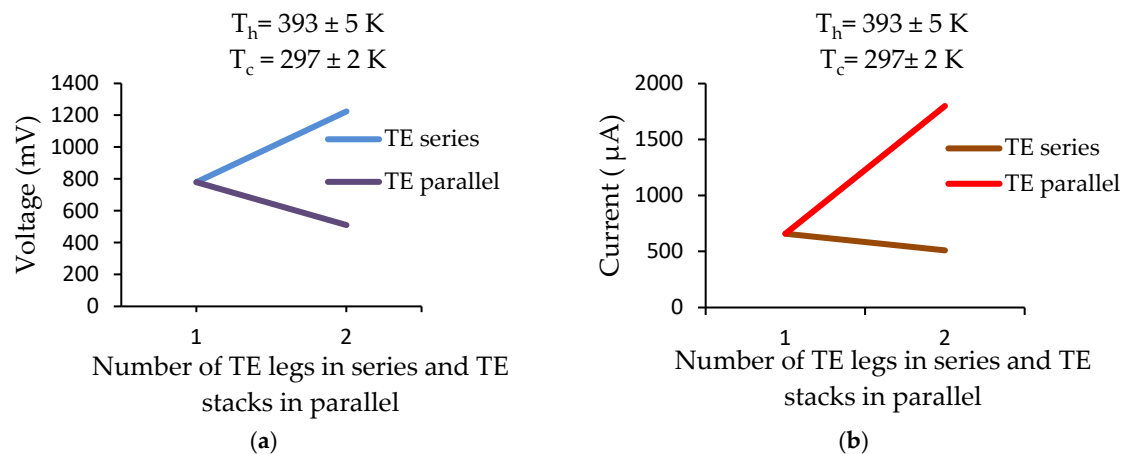


Figure 5. (a) The output voltage of the thermoelectric generator for serial and parallel connection; (b) the output current of the thermoelectric generator for serial and parallel connection.

When the modules were connected in series, the increase in the output voltage was from 780 mV (one module) to 1224 mV (two modules). The simultaneous decrease in current was measured from 658 µA (single module) to 510 µA (two modules), because the serial connection increased the internal resistance of the thermoelectric generator and as a result decreased the power of the electric current.

To reduce the internal resistance and increase the output current of the thermoelectric generator, the modules were connected in parallel. In this case, the output voltage has changed from 780 mV (single module) to 510 mV (two modules). The simultaneous increase in current was measured from 658 µA (one module) to 1800 µA (two modules), because the parallel connection decreased the internal resistance of the thermoelectric generator and as a result increased the power of the electric current.

For a given heat energy supplied, the temperature difference and the values of the output sizes (voltage, current, electric power) are influenced by the area of the common section—graphite/mixture/aluminum, by the thickness of the layer forming the mixture, and by the number and mode of connection of the thermoelectric generators. As the joint area increases, the output power also increases. An increase in the thickness of the intermediate layer increases the temperature gradient, but also the internal resistance of the thermoelectric generator. The output power of the thermoelectric generator according to the temperature of the hot plate is shown in Figure 6.

Even if the output power is small, the realization of this mixture of substances with thermoelectric properties represents a step for further research on improving the properties of the thermoelectric generator realized.

The materials used have an advantage over those commonly used, namely, they have thermal and chemical stability, are found in abundance, are cheap, have low toxicity, and are easy to process in order to obtain the thermoelement and low cost.

Figure 7 shows a graph from the technical data sheet of the commercial thermogenerator 1MD03-024-04/1, in which the variation of the electrical voltage and the electrical output power according to the temperature of the hot plate is observed [27].

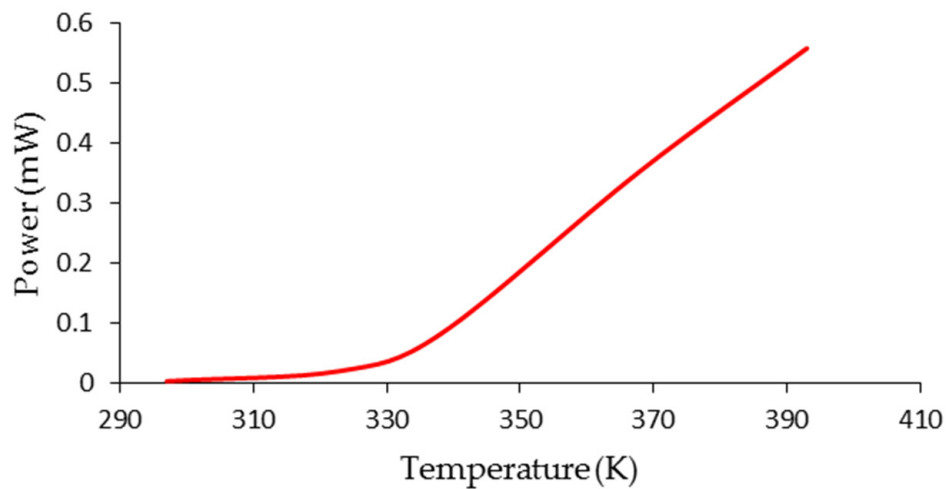


Figure 6. Output power of the thermoelectric generator.

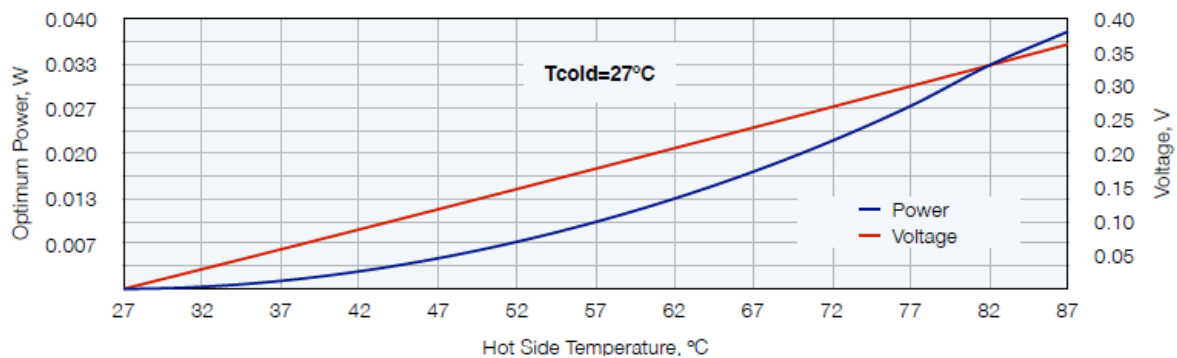


Figure 7. Voltage and power output for commercial thermoelectric generator 1MD03-024-04/1.

By connecting the thermoelectric modules in series and in parallel, it is possible to obtain values of electrical voltage and output power comparable to commercial ones.

4. Conclusions

This paper demonstrates by experimental data that the thermoelectric generator made is comparable to those produced industrially and found on the market. The originality of this research is given by the novelty of substances used to generate electric current under the action of the thermal factor.

Experimental results indicated:

- The output current and output power depends on the nature of the mixture of substances used.
- The lack of calcium hydroxide in the mixture causes fluctuations in the output current, and too much of it causes the current to decrease.
- Too much silicon dioxide causes the electric current to decrease.
- The optimum operating temperature is around 393 K.
- If an aluminum electrode is used in which a network of holes with a diameter of 0.2 mm is practiced, and it is in an environment with high humidity, then the current generated by the thermoelement increases three times.

Author Contributions: Conceptualization: M.C., A.H., H.S., and H.V.; methodology: M.C. and H.V.; validation: M.C., A.H., and H.V.; formal analysis: A.H. and H.S.; investigation: M.C.; data curation: M.C.; writing—original draft preparation: M.C.; writing—review and editing: M.C., A.H., H.S., and H.V.; visualization: A.H. and H.S.; supervision: H.V. and H.S. All authors have read and agreed to the published version of the manuscript.

Funding: This research received no external funding.

Conflicts of Interest: The authors declare no conflict of interest.

References

1. Akella, A.K.; Saini, R.P.; Sharma, M.P. Social, economical and environmental impacts of renewable energy systems. *Renew. Energy* **2009**, *34*, 390–396. [[CrossRef](#)]
2. Zheng, X.F.; Liu, C.X.; Yan, Y.Y.; Wang, Q. A review of thermoelectrics research—Recent developments and potentials for sustainable and renewable energy applications. *Renew. Sustain. Energy Rev.* **2014**, *32*, 486–503. [[CrossRef](#)]
3. Rowe, D.M. Thermoelectrics, an environmentally-friendly source of electrical power. *Renew. Energy* **1999**, *16*, 1251–1256. [[CrossRef](#)]
4. Ismail, B.I.; Ahmed, W.H. Thermoelectric Power Generation Using Waste-Heat Energy as an Alternative Green Technology. *Recent Pat. Electr. Eng.* **2009**, *2*, 27–39. [[CrossRef](#)]
5. Riffat, S.B.; Ma, X. Thermoelectric: A review of present and potential applications. *Appl. Therm. Eng.* **2003**, *23*, 913–935. [[CrossRef](#)]
6. Bulusu, A.; Walker, D.G. Review of electronic transport models for thermoelectric materials. *Superlattices Microstruct.* **2008**, *44*, 1–36. [[CrossRef](#)]
7. Elsheikh, M.H.; Shnawah, D.A.; Sabri, M.F.M.; Said, S.B.M.; Hassan, M.H.; Bashir, M.B.A.; Mohamad, M. A review on thermoelectric renewable energy: Principle parameters that affect their performance. *Renew. Sustain. Energy Rev.* **2014**, *30*, 337–355. [[CrossRef](#)]
8. Gould, C.A.; Shamma, N.Y.A.; Grainger, S.; Taylor, I. A comprehensive review of thermoelectric technology, micro-electrical and power generation properties. In Proceedings of the 2008 26th International Conference on Microelectronics, Nis, Serbia, 10–14 May 2008; pp. 329–332.
9. Snyder, G.J.; Toberer, E.S. Complex thermoelectric materials. *Nat. Mater.* **2008**, *7*, 105–114. [[CrossRef](#)]
10. Alam, H.; Ramakrishna, S. A review on the enhancement of figure of merit from bulk to nano-thermoelectric materials. *Nano Energy* **2013**, *2*, 190–212. [[CrossRef](#)]
11. Telkes, M. The efficiency of thermoelectric generators. I. *J. Appl. Phys.* **1947**, *18*, 1116–1127. [[CrossRef](#)]
12. El-Genk, M.S.; Saber, H.H.; Caillat, T. Performance tests of skutterudites and segmented thermoelectric converters. *AIP Conf. Proc.* **2004**, *699*, 541–552.
13. Shi, X.; Yang, J.; Bai, S.; Yang, J.; Wang, H.; Chi, M. On the design of high efficiency thermoelectric clathrates through a systematic cross-substitution of framework elements. *Adv. Funct. Mater.* **2010**, *20*, 755–763. [[CrossRef](#)]
14. Yang, J.; Li, H.; Wu, T.; Zhang, W.; Chen, L.; Yang, J. Evaluation of half-Heusler compounds as thermoelectric materials based on the calculated electrical transport properties. *Adv. Funct. Mater.* **2008**, *18*, 2880–2888. [[CrossRef](#)]
15. Sales, B.C.; Mandrus, D.; Williams, R.K. Filled skutterudite antimonides: A new class of thermoelectric materials. *Science* **1996**, *272*, 1325–1328. [[CrossRef](#)] [[PubMed](#)]
16. Venkatasubramanian, R.; Siivola, E.; Colpitts, T.; O’quinn, B. Thin-film thermoelectric devices with high room-temperature figures of merit. *Nature* **2001**, *413*, 597–602. [[CrossRef](#)] [[PubMed](#)]
17. Hicks, L.; Dresselhaus, M. Thermoelectric figure of merit of a one-dimensional conductor. *Phys. Rev. B* **1993**, *47*, 16631. [[CrossRef](#)] [[PubMed](#)]
18. Hicks, L.; Dresselhaus, M. Effect of quantum-well structures on the thermoelectric figure of merit. *Phys. Rev. B* **1993**, *47*, 12727. [[CrossRef](#)] [[PubMed](#)]
19. Liu, W.; Borca-Tasciuc, T.; Chen, G.; Liu, J.; Wang, K. Anisotropic thermal conductivity of Ge quantum-dot and symmetrically strained Si/Ge superlattices. *J. Nanosci. Nanotechnol.* **2001**, *1*, 39–42. [[CrossRef](#)]
20. Capinski, W.S.; Maris, H.J. Thermal conductivity of GaAs/AlAs superlattices. *Physica B* **1996**, *219*, 699–701. [[CrossRef](#)]
21. Caylor, J.; Coonley, K.; Stuart, J.; Colpitts, T.; Venkatasubramanian, R. Enhanced thermoelectric performance in PbTe-based superlattice structures from reduction of lattice thermal conductivity. *Appl. Phys. Lett.* **2005**, *87*, 023105. [[CrossRef](#)]
22. Walia, S.; Balendhran, S.; Nili, H.; Zhuiykov, S.; Rosengarten, G.; Wang, Q.H. Transition metal oxides—Thermoelectric properties. *Prog. Mater. Sci.* **2013**, *58*, 1443–1489. [[CrossRef](#)]
23. Liu, S.; Hu, B.; Liu, D.; Li, F.; Li, J.; Li, B.; Li, L.; Nan, Y.L.C. Microthermoelectric generators based on through glass pillars with high output voltage enabled by large temperature difference. *Appl. Energy* **2018**, *225*, 600–610. [[CrossRef](#)]
24. Rana, S.; Orr, B.; Iqbal, A.; Ding, L.C.; Akbarzadeh, A.; Date, A. Modelling and optimization of low-temperature waste heat thermoelectric generator system. *Energy Procedia* **2017**, *110*, 196–201. [[CrossRef](#)]

25. Chen, W.H.; Lin, Y.X. Performance comparison of thermoelectric generators using different materials. *Energy Procedia* **2019**, *158*, 1388–1393. [[CrossRef](#)]
26. Omera, G.; Yavuzb, A.H.; Ahiskac, R.; Calisald, K.E. Smart thermoelectric waste heat generator: Design, simulation and cost analysis. *Sustain. Energy Technol. Assess.* **2020**, *37*, 100623. [[CrossRef](#)]
27. RMTLtd Thermoelectric Cooling Solutions. Available online: <http://www.rmtltd.ru/applications/temicrogenerators> (accessed on 5 February 2020).

Publisher’s Note: MDPI stays neutral with regard to jurisdictional claims in published maps and institutional affiliations.



© 2020 by the authors. Licensee MDPI, Basel, Switzerland. This article is an open access article distributed under the terms and conditions of the Creative Commons Attribution (CC BY) license (<http://creativecommons.org/licenses/by/4.0/>).